

Direct Observation of Charge Transfer  
 at Jahn-Teller Transition in a Perovskite  $\text{RbMn}[\text{Fe}(\text{CN})_6]$ 

Transition metal cyanides,  $A(\text{I})M(\text{II})[\text{N}(\text{III})(\text{CN})_6]$  ( $A = \text{Na, K, Rb, Cs}$ ;  $M = \text{Mn, Co, Cr}$ ;  $N = \text{Fe, Cr}$ ), have been attracting the renewed interest of materials scientists, because they show a novel photoinduced magnetization/demagnetization in addition to the thermally induced spin-state transition. They also have the characteristic structure: the transition metal ions are surrounded by six cyanos ( $\text{CN}^-$ ) and form a three-dimensional — $M\text{-NC-N}$ — network analogous to the double-perovskite-type transition metal oxides. In this sense, the study of the transition metal cyanides will contribute to a deeper comprehension of the strongly correlated electron system. Most of the transition metal cyanides, however, contain considerable nonstoichiometric  $\text{H}_2\text{O}$  molecules, which make the structural analysis difficult. Among the transition metal cyanides,  $\text{RbMn}[\text{Fe}(\text{CN})_6]$  [1] does not contain extra  $\text{H}_2\text{O}$  molecules and is suitable for precise structural analysis on the charge density level. Ohkoshi *et al.* [1] observed temperature-induced cubic ( $F4-3m$ ;  $Z = 4$ ) tetragonal ( $I4-m2$ ;  $Z = 2$ ) transition at around 220 K. The structural transition is ascribed to the charge transfer from the  $\text{Mn}^{2+}$  site to the  $\text{Fe}^{3+}$  site, because the resultant Jahn-Teller distortion of  $\text{Mn}^{3+}$  ( $d^4$ ) can cause the tetragonal structure [2]. With a further decrease in temperature below 12 K ( $= T_C$ ), the local spins at the Mn sites are ferromagnetically ordered, as confirmed by neutron powder diffraction experiment [3]. Tokoro *et al.* [4] observed the suppression of magnetization by a visible pulse laser irradiation at 3 K.

To obtain X-ray powder data of good counting statistics with high angular resolution, measurements were carried out at beamline **BL02B2**. The as-grown sample powders were sealed in a 0.3 mm  $\phi$  Lindemann capillary, which gave a homogeneous intensity distribution in the Debye-Scherrer powder ring. The wavelength of the incident X-ray was 0.82 Å (slightly longer than the  $K$ -edge of Rb), and the exposure times were 26 min at 300 K and 67 min at 92 K.

The electron density distributions at both temperatures were visualized by the maximum entropy method (MEM) combined with the Rietveld refinement. The MEM analysis was carried out with a program ENIGMA using  $100 \times 100 \times 100$  pixels ( $72 \times 72 \times 108$  pixels) at 300 K (at 92 K). In Fig. 1, the MEM charge density of the

(100) section containing Mn, Fe, C, and N atoms is shown at 300 K with schematics of crystal structure. The contour lines are drawn only for the lower density region ( $4.0 \text{ e}\text{\AA}^{-3}$ ). The MEM charge density clearly exhibits the Mn-N and the Fe-C bonding features. The charge density distribution is isotropic around  $\text{Mn}^{2+}$  because both the  $e_g$  orbitals, that is,  $dx^2 - y^2$  and  $d3z^2 - r^2$ , are occupied in the cubic phase. The minimum of the charge density ( $= 0.80 \text{ e}\text{\AA}^{-3}$ ) in the Fe-C bond is larger than that ( $= 0.60 \text{ e}\text{\AA}^{-3}$ ) in the Mn-N bond. This bonding electron distribution is consistent with the picture that  $\text{RbMn}[\text{Fe}(\text{CN})_6]$  consists of  $\text{Fe}(\text{CN})_6$  complexes and cations ( $\text{Rb}^+$  and  $\text{Mn}^{2+}$ ). The charge density distribution markedly changes at the cubic-tetragonal transition. Figure 2(a) shows the MEM charge density of  $\text{RbMn}[\text{Fe}(\text{CN})_6]$  for the (110) section at 92 K. One may notice that the charge density distribution around Mn becomes anisotropic: the minimum of the charge density ( $= 0.65 \text{ e}\text{\AA}^{-3}$ ) in the Mn- $N_{xy}$  bond is higher than that ( $= 0.28 \text{ e}\text{\AA}^{-3}$ ) in the Mn- $N_z$  bond. Obviously, this anisotropy is attributed to the charge transfer from the  $\text{Mn}^{2+}$  site to the  $\text{Fe}^{3+}$  site, which causes a hole on the  $e_g$  orbital of the Mn ion.

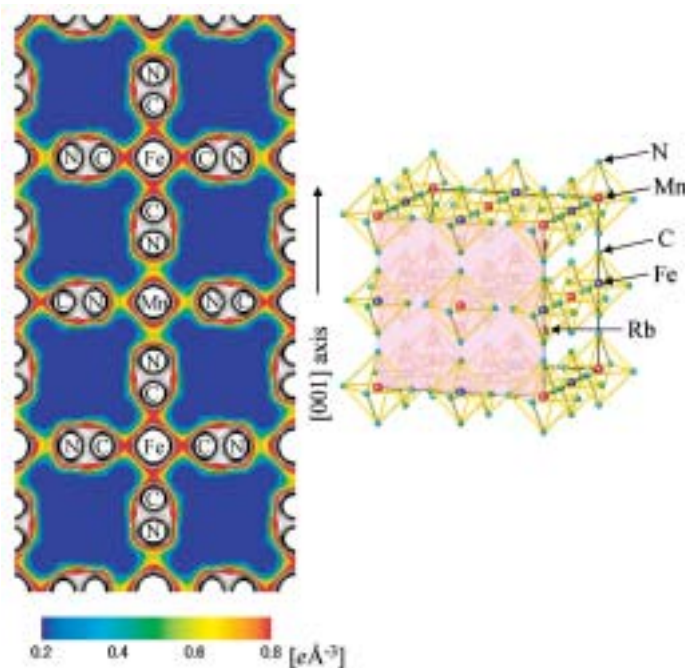


Fig. 1. MEM electron density distribution of  $\text{RbMn}[\text{Fe}(\text{CN})_6]$  for the (100) section at 300 K in the high-temperature cubic phase ( $F4-3m$ ;  $Z = 4$ ). Contour lines are drawn from 0.0 to  $4.0 \text{ e}\text{\AA}^{-3}$  at intervals of  $0.2 \text{ e}\text{\AA}^{-3}$ . A schematic shows the crystal structure.

It is interesting to investigate the variation of the charge densities around the Mn ion and the Fe ion at the cubic-tetragonal transition. Figure 3 shows the charge density of RbMn[Fe(CN)<sub>6</sub>] along the Mn-NC-Fe bond at 300 and 92 K. The charge density around the Mn ion significantly decreases in the tetragonal phase. We estimated the total charges around the Mn ion by spherical integration up to the midpoint of the Mn-N bond, i.e., 1.09 Å for the cubic phase and 1.06 Å for the tetragonal phase. The total charge decreases from 23.0(2)*e* to 22.2(2)*e* at the cubic-tetragonal transition, indicating the valence change from Mn<sup>2+</sup> to Mn<sup>3+</sup>.

We have calculated the charge density distribution with the full-potential linearized augmented plane-wave method within the local density approximation (LDA) scheme. The actual tetragonal lattice parameters at 92 K determined by Rietveld analysis were used. The calculated spin moment  $\mu_{\text{Mn}}$  at the Mn site (= 3.2  $\mu_{\text{B}}$ ) is nearly consistent with the experimental results [ $\mu_{\text{Mn}} = 3.2(7) \mu_{\text{B}}$  [3]]. Figure 2(b) shows the calculated charge density of RbMn[Fe(CN)<sub>6</sub>] for the (110) section. Heights and interval of the contour lines are the same for both the experimental [Fig. 2(a)] and calculated [Fig. 2(b)] images. The LDA calculation quantitatively reproduces the MEM charge density, including the anisotropic charge density around Mn<sup>3+</sup>.

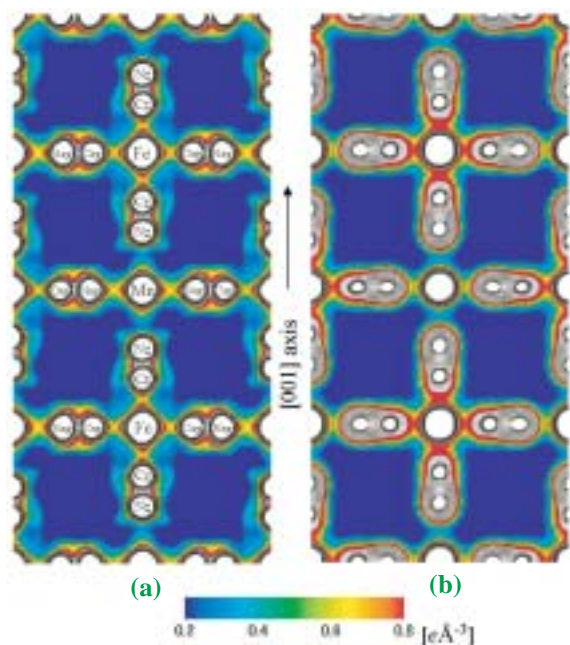


Fig. 2. (a) MEM electron density distribution of RbMn[Fe(CN)<sub>6</sub>] for the (110) section in the low-temperature tetragonal phase (*I4-m2*; *Z* = 2) at 92 K. (b) Electron density distribution of RbMn[Fe(CN)<sub>6</sub>] for the (110) section determined by the LDA first-principles calculation based on the actual atomic coordinates. Contour lines are drawn from 0.0 to 4.0  $e\text{\AA}^{-3}$  at intervals of 0.2  $e\text{\AA}^{-3}$ .

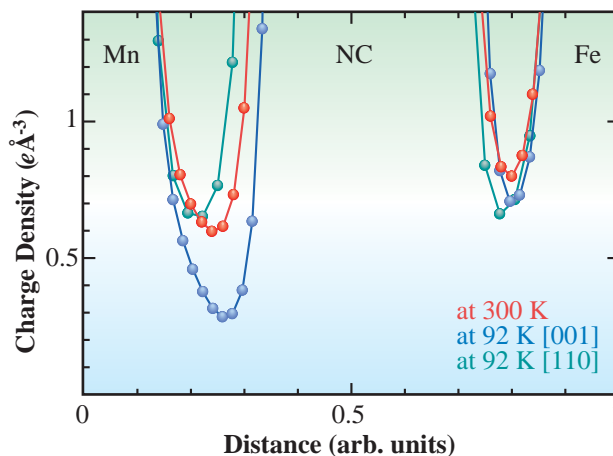


Fig. 3. Charge density of RbMn[Fe(CN)<sub>6</sub>] along the Mn-NC-Fe bond at 300 and 92 K, determined by MEM/Rietveld analysis.

Actually, the calculated minima of the charge densities are 0.59  $e\text{\AA}^{-3}$  and 0.32  $e\text{\AA}^{-3}$  in the Mn-N<sub>xy</sub> and Mn-N<sub>z</sub> bonds, respectively, which are close to the experimentally obtained values (0.65  $e\text{\AA}^{-3}$  and 0.28  $e\text{\AA}^{-3}$  in the Mn-N<sub>xy</sub> and Mn-N<sub>z</sub> bonds, respectively).

In summary, we have investigated the variation of charge density at the Jahn-Teller transition of RbMn[Fe(CN)<sub>6</sub>] and directly observed the charge transfer from the Mn site to the Fe site at the cubic-tetragonal transition [5]. We further interpreted the anisotropic charge density distribution around Mn<sup>3+</sup> in terms of the bonding electrons. Thus, the MEM/Rietveld charge density analysis proved to be effective for the deeper comprehension of the transition metal compounds.

Kenichi Kato<sup>a</sup> and Yutaka Moritomo<sup>b</sup>

(a) JASRI / SPRING-8

(b) Department of Applied Physics, Nagoya University

E-mail: katok@spring8.or.jp

## References

- [1] S. Ohkoshi *et al.*: J. Phys. Chem. B **106** (2002) 2423.
- [2] Y. Moritomo *et al.*: J. Phys. Soc. Jpn. **71**(2002) 2078.
- [3] Y. Moritomo *et al.*: J. Phys. Soc. Jpn. **72** (2003) 456.
- [4] H. Tokoro *et al.*: Appl. Phys. Lett. **82** (2003) 1245.
- [5] K. Kato, Y. Moritomo, M. Takata, M. Sakata, M. Umekawa, N. Hamada, S. Ohkoshi, H. Tokoro, K. Hashimoto: Phys. Rev. Lett. **91** (2003) 255502.